Desalination and Water Treatment
www.deswater.com

doi: 10.5004/dwt.2019.23764

151 (2019) 242–250
May

Removal of As(V) and As(III) species from wastewater by adsorption on coal fly ash

Yulong Wang[a,b,*], Shaofeng Wang[b,*], Guoqing Zhang[b], Xin Wang[b], Shuyan Zang[c,*], Yongfeng Jia[b]

[a]*Key Laboratory of Geospatial Technology for the Middle and Lower Yellow River Regions, College of Environment and Planning, Henan University, Kaifeng, 475004, China, Tel./Fax: +86 371 23881939; email: 10130133@vip.henu.edu.cn (Y. Wang)*
[b]*Key Laboratory of Pollution Ecology and Environmental Engineering, Institute of Applied Ecology, Chinese Academy of Sciences, No. 72, Wenhua Road, Shenyang, 110016, China, Tel./Fax: +86 24 8397 0503; emails: wangshaofeng@iae.ac.cn (S. Wang), 18624714965@163.com (G. Zhang), wangxin@iae.ac.cn (X. Wang), yongfeng.jia@iae.ac.cn (Y. Jia)*
[c]*Shenyang University of Chemical Technology, Shenyang, 110142, China, Tel./Fax: +86 24 89383297; email: zangshuyan@126.com*

Received 19 July 2018; Accepted 8 January 2019

ABSTRACT

Arsenic is ubiquitous in many natural systems and poses great risk to human health. Coal fly ash is a waste by-product of thermal power plants that may cause serious environmental problems. To reduce environmental hazards and realize high-value utilization of coal fly ash, it was characterized using the scanning electron microscopy, Brunauer–Emmet–Teller, and powder X-ray diffraction methods, and the arsenate (As(V)) and arsenite (As(III)) removal performance of coal fly ash used as an adsorbent from aqueous solutions was investigated using batch experiments. Adsorption kinetics study revealed that the adsorption of As(V) and As(III) by fly ash was fast in the first 4 h and equilibrium was achieved within 48 h at pH 5.0 with an initial arsenic concentration of 1 mg/L and an adsorbent dose of 4 g/L. The adsorption kinetics are well described by the pseudo-second-order rate equation model, with high coefficients of determination (R^2) of 0.9991 and 0.9925 for As(V) and As(III) adsorption, respectively. The Langmuir adsorption isotherms of arsenic adsorption indicated that the highest adsorption capacities of As(V) and As(III) at pH 5.0 were 666.67 and 232.56 mg/kg, respectively. The results of the arsenic adsorption edges conducted at different pH values from 3 to 11 with initial arsenic concentration of 1 mg/L and adsorbent dose of 4 g/L revealed that the removal of As(V) was obviously more than that of As(III) under the same conditions, with respect to the same pH. Different from the sharp maximum adsorption at pH around 5.0 on the As(V) adsorption edge, the As(III) adsorption maximum is broad, occurred in the pH range of approximately 5.0 to 7.0. The significant differences in the adsorption of As(V) and As(III) on fly ash could be due to the discrepant electrostatic interaction between Al-based hydroxyl groups on the surface of fly ash and arsenic species in aqueous solution. Furthermore, this approach provides a possible method for treating arsenic wastewater and potential application for the reuse of coal fly ash generated by other industrial activities.

Keywords: Arsenic; Arsenate; Arsenite; Coal fly ash; Adsorption; Reuse

* Corresponding authors.

1944-3994/1944-3986 © 2019 Desalination Publications. All rights reserved.

1. Introduction

Arsenic (As), one of the most toxic and carcinogenic chemical elements, is present in virtually every part of the environment, including the atmosphere, soil, rocks, water, and food, and has become a worldwide problem for human health [1–7]. Long-term exposure to arsenic-contaminated drinking water can lead to lung, liver, skin, kidney, and bladder cancers as well as hypertension and cardiovascular disease [8]. Due to its high toxicity and accumulation, the World Health Organization (WHO) and many countries, such as the United States and China, have set a guideline limit of 10 $\mu g \cdot L^{-1}$ for the arsenic content in public drinking water, leading to an urgent need to develop an improved arsenic removal processes in water treatment systems in order to meet the stringent drinking water standards [9].

To date, various treatment technologies for arsenic removal, such as adsorption, chemical coagulation-precipitation, electrodialysis, reverse osmosis, ion-exchange, membrane separation, and biological treatments, have been developed and compared [2,10–24]. Among these methods, adsorption is usually considered to be the most attractive technology because of its relatively low cost, high efficiency and convenient operation [20,25–28]. Fe- or Al- oxyhydroxides have been systematically studied and widely used as adsorbents for arsenic removal due to their abundance in the environment, high affinity for arsenic species and low operating costs [10,12,29–41]. Macroscopic and spectroscopic techniques, such as synchrotron X-ray absorption and ATR-FTIR spectroscopies, have been employed extensively to investigate the molecular-scale adsorption mechanisms of arsenate and arsenite on a range of natural and synthetic minerals (such as goethite and 6-L ferrihydrite) [33–35,42]. According to these studies, both As(V) and As(III) are strongly adsorbed on metal oxyhydroxide surfaces, forming predominantly inner-sphere surface complexes by ligand exchange reactions and resulting in either monodentate or binuclear bidentate complexes depending on the surface arsenic loading and solution chemistry.

With the increased electric power consumption, a great amount of coal fly ash (a by-product of coal fired electricity generation) has been produced in recent decades [43,44]. Despite a large fraction of the volume of the generated coal fly ash has been reused, benefiting applications such as cement manufacturing, structural fillers, and waste stabilization, amount representing millions of tons are stored in ash impoundments. This fly ash not only wastes a large amount of land but also contaminates the environment [45]. Specially, the failure of ash impoundment structures and the toxic chemicals of the fly ash have highlighted the risk to environmental systems and drinking water sources [46,47]. In order to protect and optimize the consumption of natural resources, coal fly ash and modified coal fly ash have been studied for decades as sorbents for removing heavy metals and organic pollutant from wastewater [48–55]. Up to now, to the best of our knowledge, these studies have focused on the arsenate adsorption characteristics and removal mechanisms of arsenic by fly ash and/or modified coal [56–60]. However, even though both As(V) and As(III) species are usually present in wastewater and groundwater, studies of As(III) adsorption performance by fly ash are lacking [1,2].

Therefore, the main objectives of this study were (1) to characterize the coal fly ash using powder X-ray diffraction (p-XRD) patterns, N_2 adsorption–desorption isotherms (Brunauer–Emmet–Teller [BET]) and scanning electron microscopy (SEM), and (2) to investigate its performance in the removal of As(V) and As(III) species using batch experiments.

2. Material and methods

2.1. Materials

All of the chemicals used in this work were of analytical or guarantee reagent grade, were purchased from commercial sources and were used without further purification. As_2O_5, As_2O_3 $Fe(NO_3)_3 \cdot 9H_2O$ and NaOH were of analytical grade, HCl and HNO_3 were of guarantee grade, and all were purchased from Sigma-Aldrich. As_2O_5 dissolves easily in water and alcohol, but this process takes a long time. However, As_2O_3 is lower soluble in pure water, but has higher solubility and a faster dissolution rate in NaOH solution. All solutions except for the As_2O_3 solution were prepared in deionized water. All of the volumetric flasks and vessels were cleaned by soaking in 5% HNO_3 for at least 12 h and were rinsed several times with distilled water prior to the tests. The artificial stock solutions of As(III) and As(V) for batch studies were made by dissolving As_2O_3 in NaOH solution and As_2O_5 in deionized (DI) water, respectively. The concentrations of the arsenic stock solutions were determined using a hydride-generation atomic fluorescence spectrophotometer (AFS-3100, Haiguang Corp., Beijing) prior to adsorption experiments. The arsenic working solutions were freshly prepared by diluting the stock arsenate solutions with deionized water.

The commercial coal fly ash used in this study was obtained from Jining Hengzhi New building materials, Ltd. (Jining, China) and had the typical chemical composition of fly ash, as summarized in Table 1. Prior to the experiments, the fly ash was washed by soaking in 6 M HNO_3 solution at room temperature for 24 h, then was separated by centrifugation, washed several times by distilled water, and dried in an oven at 60°C overnight.

2.2. Batch adsorption experiments

Arsenic removal by the fly ash was conducted by addition of the solid to the arsenic solutions at room temperature (25°C ± 1°C). The solution pH was adjusted to the target value

Table 1
Most probable oxide calculation for the fly ash in this study, performed using mineral recalculation software

Element as oxide	Percentage (wt %)
SiO_2	45.85
Al_2O_3	27.52
CaO	6.78
Fe_2O_3	5.71
K_2O	2.65
TiO_2	1.49

by addition of NaOH and/or HCl solution before the addition of the adsorbent. All batch experiments were performed in duplicate, and the mean values were used to analyze the results of the study. The uptake of arsenic by the fly ash was determined based on the difference between the initial and final arsenic concentrations in the solution divided by the weight of the adsorbent.

2.2.1. Adsorption kinetics

The rate of arsenic adsorption is an important factor for arsenic removal. Batch experiments were performed to determine the reaction time necessary to reach the adsorption equilibrium; 1.0 g fly ash adsorbent was added to the conical flasks containing 250 mL of 1.0 mg/L arsenic solution. The initial pH of the solution was adjusted to 5.0 ± 0.2 with 0.1 M HCl or 0.1 M NaOH and was maintained at the same pH value throughout the adsorption process. Then, the mixture was shaken on a platform shaker with an agitation speed of 180 rpm at the temperature of 25°C ± 1°C. Approximately, 3 mL aliquots were taken from the vessel at selected reaction time intervals as follows: 0.083, 0.25, 0.5, 1, 3, 6, 8, 12, 24, 30, 36, and 48 h. The samples were immediately filtered through a 0.22 μm membrane filter (Millipore) for the analysis of aqueous arsenic concentration.

2.2.2. Arsenic adsorption edges

To investigate the influence of pH on arsenic adsorption by fly ash, batch experiments were carried out by adding 0.4 g of the adsorbent sample into 100 mL of 1.0 mg/L arsenic solution for 48 h. The vessels were shaken in an orbit shaker at 180 rpm for 48 h at 25°C ± 1°C. The pH of the system was kept constant at the target value by addition of NaOH and/or HCl solution. At the end of the experiments, the mixtures were allowed to settle, and the supernatant was passed through a 0.22 μm membrane (Millipore) with a syringe filter to determine the residual arsenic concentrations in the supernatant solutions.

2.2.3. Arsenic adsorption isotherms

Adsorption isotherms were measured to estimate the maximum adsorption density. To obtain adsorption isotherms, the initial As(V) or As(III) concentrations were 1.0, 2.0, 3.0, 4.0, 5.0, 6.0, 7.0, 8.0, and 9.0 mg/L, respectively, and the pH of the solution was adjusted to 5.0 ± 0.2 by the addition of 0.1 M HCl or NaOH. Then, 0.4 g absorbent was added to each solution. Afterwards, the suspensions were shaken on an orbit shaker at 180 rpm for 48 h. The slurries were maintained at pH 5.0 ± 0.2 by the addition of 0.1 M HCl or NaOH. Finally, the supernatant was filtered through a 0.22 μm membrane filter after the solutions were mixed for 48 h.

2.3. Analytical methods

The concentrations of As(V) and As(III) in solution were measured using a hydride-generation atomic fluorescence spectrophotometer (AFS-3100, Haiguang Corp., Beijing) with a detection limit of 0.1 μg/L, and duplicate analyzes agreed within 5%, according to previously reported procedures [61,62]. The samples were pretreated with an ascorbic acid/thiourea reducing agent (5 g of thiourea and 5 g of ascorbic acid in 100 mL of H_2O) to reduce all arsenic to As(III) prior to hydride generation. The borohydride solution was prepared by dissolving 10 g of KBH_4 in 500 mL of 0.5% (w/v) NaOH solution and was used as the reducing agent for AsH_3 generation. A 5% HCl solution was used as the carrier solution. All samples were analyzed within 24 h of collection, and an appropriate dilution had been made for higher As concentrations using the 5% HCl solution before As concentrations in solution were analyzed.

The morphological structures and elemental compositions of the coal fly ash before or after the arsenic adsorption were examined by SEM (S-3400N, Hitachi, Japan). p-XRD patterns were recorded with a Rigaku Miniflex II diffractometer using Cu*Kα* radiation to determine the probable oxide components of the fly ash used in this investigation. The powder diffraction data of quartz (SiO_2) and mullite ($3Al_2O_3{\cdot}2SiO_2$) was obtained from the RRUFF Project website via <http://rruff.info/>, with RRUFF R141101 for mullite and RRUFF R110108 for quartz. The BET specific surface area, pore size distribution and pore volume of the fly ash were determined by the N_2 adsorption–desorption isotherm using a NOVA 3000 BET analyzer (ASAP 2010M, Micrometritics, USA), which are given in Table 2. The laser particle size (LPS) technology was used to analyze the particle size distribution of the material using a laser particle sizer (Nano ZS, UK).

The point of zero charge (pH_{PZC}) of the fly ash was estimated according to the method described by Yu et al. [13]. In detail, the fly ash was first suspended in 0.01 M NaCl until the pH no longer changed appreciably. Then, the pH of the suspension was adjusted to a series of pH values between 3 and 11 by adding NaOH or HCl. After equilibration for 2 h, the initial pH was recorded. Then, 1.5 g NaCl was added into each suspension and the final pH was measured after additional 3 h. The pH_{PZC} was identified as the point at which the ΔpH is equal to 0 in the curve of ΔpH vs. the final pH. ΔpH was calculated as the difference between the final pH and the initial pH.

3. Results and discussion

3.1. Characterization of the adsorbent

The powder X-ray diffraction pattern of the fly ash is illustrated in Fig. 1(a). The main peaks of fly ash were assigned to quartz (SiO_2) and mullite ($3Al_2O_3{\cdot}2SiO_2$). The wide diffraction peak between 15° and 30° reveals that a large amount of the amorphous phase is present in fly ash. Fig. 1(b) illustrates the nitrogen adsorption–desorption isotherm of the fly ash. The curve is close to the *x*-axis at relatively low pressures, indicating that the adsorption isotherms followed the type

Table 2
BET specific surface area, pore size, pore volume, and average particle size of the fly ash

Specific surface area (m^2/g)	12.32
Pore size (nm)	4.17
Pore volume (cm^3/g)	0.032
Average particle size (μm)	5.75

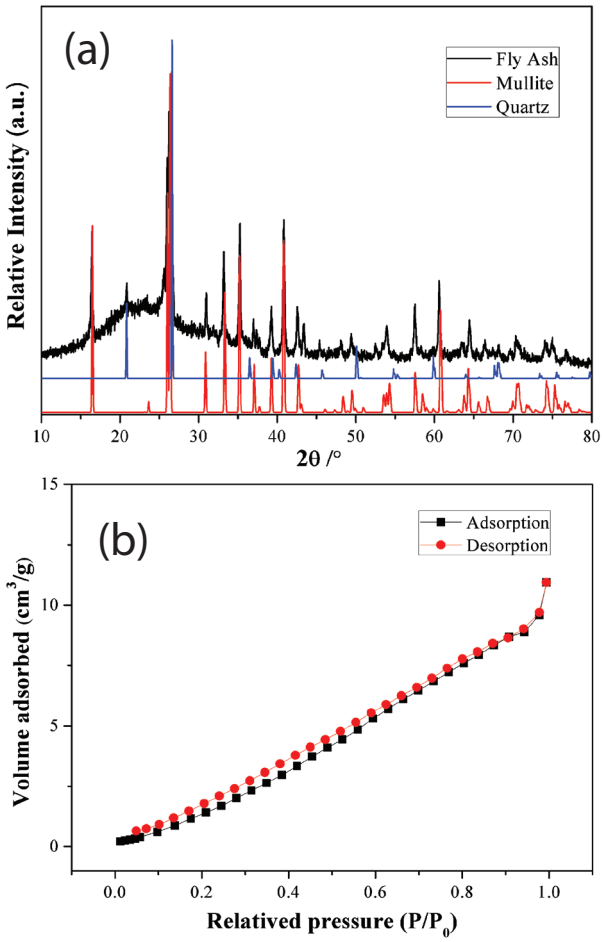

Fig. 1. (a) Powder X-ray diffraction pattern of the fly ash, compared with the powder diffraction patterns of quartz (SiO_2) and mullite ($3Al_2O_3{\cdot}2SiO_2$) obtained from the RRUFF Project website. The RRUFF IDs for quartz and mullite are R110108 and R141101, respectively. (b) Nitrogen adsorption–desorption isotherm of fly ash.

III isotherm based on the BDDT classification. This result indicated the presence of a weak interaction between the N_2 and fly ash during the multilayer adsorption. Additionally, according to the BET method, fly ash showed a specific surface area of 12.32 m^2/g, a pore volume of 0.032 cm^3/g, and a mean pore diameter of 4.17 Å, as shown in Table 2. LPS analysis shows that the mean particle size of fly ash is 5.75 μm. The morphology of the fly ash was examined by SEM. As shown in Fig. 2, the fly ash was composed of spherical particles and the main particle size of fly ash is in the range of 1.5–8 μm, which is comparable to the results of LPS analysis.

3.2. Adsorption kinetics

Kinetic experiments were performed to determine the rate of arsenic removal from water by the adsorbent. The kinetics of As(V) and As(III) removal by the fly ash were conducted by adding 4.0 g/L fly ash to a solution of 1.0 mg/L arsenic at pH 5.0 at room temperature and pressure and the results are shown in Fig. 3(a). It is clear that the arsenic adsorption process can be divided into two steps: the first relatively rapid

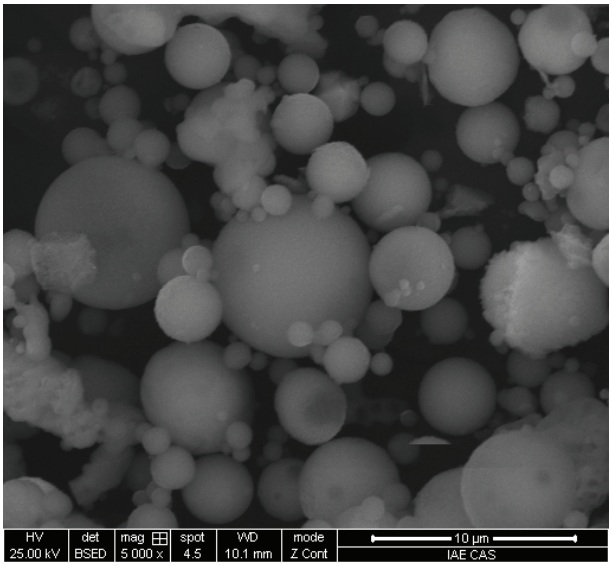

Fig. 2. SEM micrograph (′5,000) of fly ash.

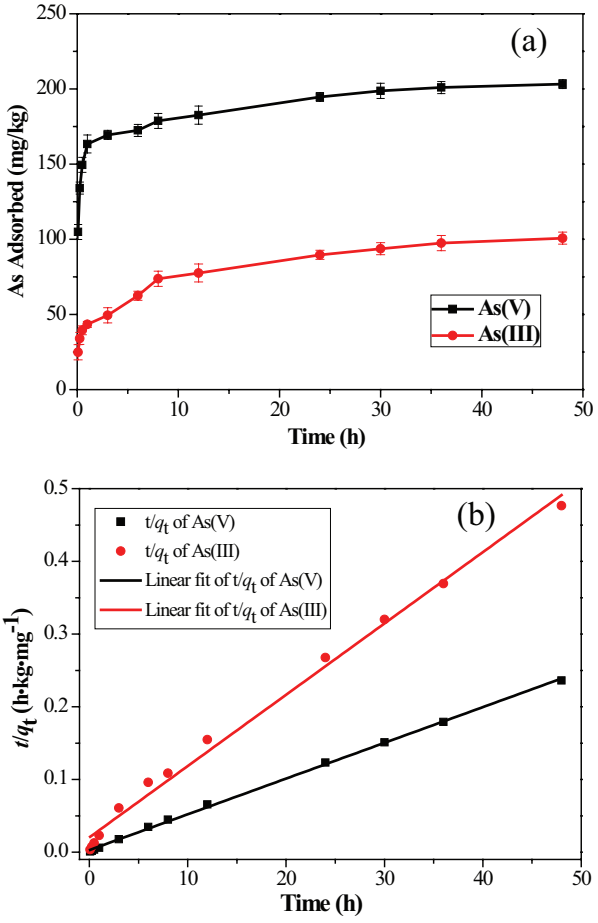

Fig. 3. Adsorption kinetics of As(III) and As(V) by fly ash (a) and their fit with a pseudo second-order rate model (b). Experimental conditions: pH 5.0 ± 0.1, adsorbent dose = 4.0 g/L, initial arsenic concentrations C_0 = 1.0 mg/L, and equilibration time, 48 h.

adsorption step, and followed by a slower adsorption process. For the As(V) adsorption kinetics, the arsenic removal in solution was extremely fast during the initial 4 h, and over 80% of the equilibrium adsorption capacity was removed. In the following adsorption step, surface precipitation and intraparticle diffusion dominate the arsenic adsorption kinetics [32,35,63]. Therefore, the adsorption rate decreased and the system reached an equilibrium state within 36 h. Thus, for all other batch experiments, the equilibration time of 48 h that was higher than the equilibrium time of 36 h was applied to ensure complete adsorption. Similar trends, but with lower adsorption capacities, were observed for the uptake of As(III) by fly ash. Such analogous adsorption kinetics by Fe-, Mn-, and Al- oxyhydroxides have also been reported previous in the literature [10,12,29,33,34]. The pseudo-second-order rate equation model was applied to describe the As adsorption kinetic data in order to investigate the mechanism of As adsorption on fly ash. The adsorption constant (K_C, kg/(mg·h)) can be calculated using the following equation:

$$\frac{t}{q_t} = \frac{1}{K_c q_e^{\,2}} + \frac{t}{q_e} \tag{1}$$

where q_t (mg/kg) is the amount of adsorption at time t and q_e (mg/kg) is the amount of adsorption at equilibrium [64].

The plots of t/q_t vs. t for both As(III) and As(V) are shown in Fig. 3(b) and the parameters obtained from the kinetic model are listed in Table 3. Remarkably, the data for As(III) and As(V) adsorption are fit well by the pseudo-second-order equation model, with high coefficients of determination (R^2) of 0.9991 and 0.9925 for As(V) and As(III) adsorption, respectively. Furthermore, the removal of As(III) and As(V) at equilibrium q_e values calculated from the pseudo-second-order equation model are 203.25 and 101.94 mg/kg, respectively, which are in good agreement with the results from the batch isotherm study (Fig. 5).

3.3. Effect of absorbent dosage

Since the arsenic removal by adsorption is highly affected by the adsorbent dosage, the effect of the adsorbent dosage on the uptake of As(V) and As(III) by fly ash was studied and the results are depicted in Fig. 4. It can be seen that the removal efficiency of both As(V) and As(III) increased from approximately 15.6% and 12.5% to 97.6% and 95.6%, respectively, as the adsorbent dosage of fly ash increased from 1.0 to 10.0 g/L, respectively. This increase could be attributed to the increase in the number of exchangeable sites and the surface area at higher concentrations of the absorbent [12,42]. When the concentration of fly ash in solution was 4.0 g/L, the adsorption capacity of fly ash for As(V) removal was approximately 81.3%, compared with the adsorption capacity for As(III) removal of 40.4%. Therefore, the adsorbent dose of fly ash of 4.0 g/L was applied in all of the subsequent adsorption tests.

Table 3
Kinetic parameters for arsenate and arsenite adsorption by Fe-modified molecular sieves using a pseudo-second-order equation model

Parameters	q_e (mg/kg)	Kc (kg/[mg·h])	R^2
As(V)	203.25	8.35×10^{-3}	0.9991
As(III)	101.94	4.73×10^{-3}	0.9925

3.4. Adsorption isotherms

Arsenic adsorption isotherms obtained at pH 5.0 were used to evaluate the adsorption capacities of fly ash and are presented in Fig. 5. It is clear that much more arsenate than arsenite was removed by fly ash from the arsenic solution, consistent with the arsenic adsorption edges (Fig. 6). The Langmuir isotherm model was employed to quantitatively describe the effect of increased aqueous As concentrations on the surface loadings of As(III) and As(V) on fly ash. The linear form of Langmuir equation is expressed as follows:

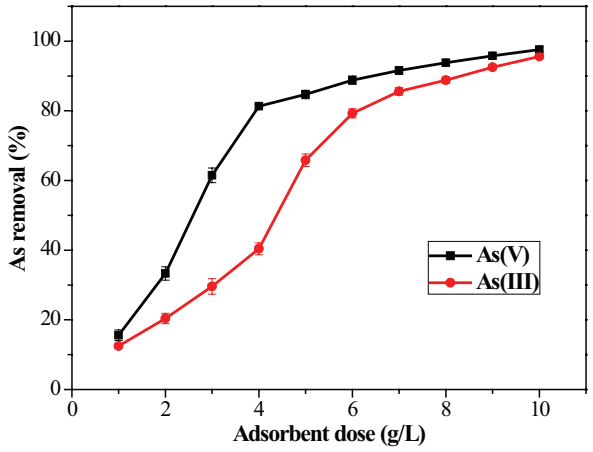

Fig. 4. Effect of the adsorbent dosage on arsenic removal by fly ash from As(V) and As(III) solutions, respectively. Experimental conditions: initial arsenic concentrations C_0 = 1 mg/L, pH 5.0 ± 0.1, temperature, 25°C, and equilibration time of 48 h.

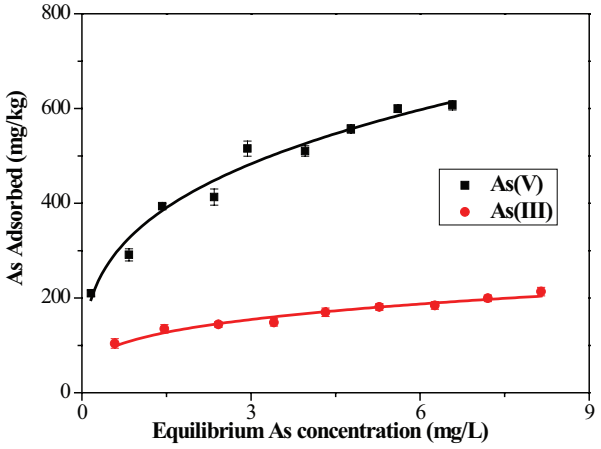

Fig. 5. As(V) and As(III) sorption isotherms for the Fe-modified molecular sieves. The solid line is the Langmuir fit to the experiment data. Experimental conditions: adsorbent dose = 4.0 g/L, pH = 5.0 ± 0.1, and equilibration time of 48 h.

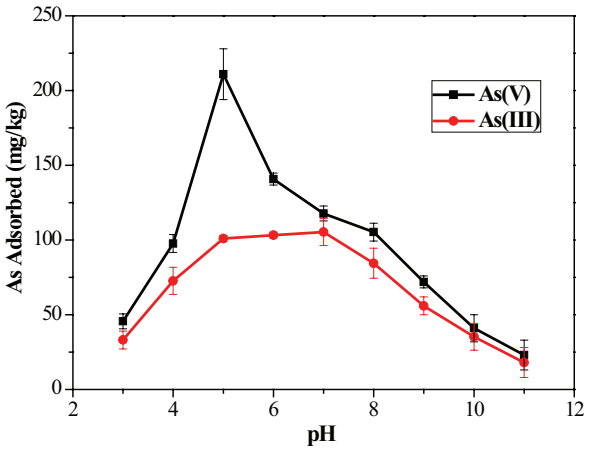

Fig. 6. Comparison of the As(V) and As(III) adsorption edges on fly ash. Experimental conditions: adsorbent dose = 4.0 g/L, initial arsenic concentrations C_0 = 1.0 mg/L, and equilibration time of 48 h.

$$\frac{C_e}{q_e} = \frac{1}{q_{\max}} C_e + \frac{1}{bq_{\max}} \quad (2)$$

where q_e (mg/kg) is the amount of As adsorption, $q_{\max}$ (mg/kg) is the maximum amount of adsorbed As ions per unit weight of the adsorbent for a complete monolayer coverage, C_e (mg/L) is the equilibrium concentration in the solution phase, and b (L/mg) is the equilibrium adsorption constant, which represents the free energy of adsorption.

As a result, the maximum adsorption amounts of As(V) and As(III) from solution were calculated from the Langmuir equation and used as the arsenic adsorption capacity. The adsorption constants obtained from the Langmuir isotherm model at our experimental conditions are given in Table 4. As shown in Table 4, high regression coefficients ($R^2 > 0.97$) suggested that the Langmuir model was suitable for describing the arsenic adsorption behavior of fly ash. The calculated As(V) and As(III) adsorption capacities were 666.67 and 232.56 mg/kg, respectively. This indicates that monolayer adsorption plays a key role in arsenic removal. A comparison of arsenic adsorption capacities has been performed for other reported fly ash-based adsorbents [59,65]. It has been reported that the capacity of iron-containing fly ash for arsenate adsorption is 19.46 mg/kg [65], which could be ascribed to the higher BET specific surface area and/or iron content.

3.5. Adsorption edges

The pH of the solution is one of the most important factors in the treatment of groundwater for arsenic, for the pH could affect the surface charge of the adsorbents and the speciation of arsenic. Therefore, it is necessary to investigate the effect of pH on the arsenic adsorption process. The results of the adsorption edges of As(V) and As(III) on fly ash in the pH range from 3 to 11 at pH 5.0 with a reaction time of 48 h are shown in Fig. 6. As can be seen, the uptake of As(V) by fly ash was remarkably higher than that of As(III) under the same conditions, with respect to the same pH value, which could be due to the differences in the absorbent surface properties and adsorption behaviors of As(V) and As(III). It has been reported by previous literatures that the adsorption of As(V) on ferrihydrite and goethite is more favorable than that of As(III) under acidic conditions, whereas above pH 7–8, As(III) has a higher affinity onto the solids [10,12]. Different from arsenic removal by ferrihydrite and other iron-based absorbents, the removal efficiency values of As(III) by aluminium-based absorbents, such as Friedel's salt ($3CaO{\cdot}Al_2O_3{\cdot}CaCl_2{\cdot}10H_2O$) [66], mesoporous alumina [30], coagulant polyaluminium chloride [31], polyaluminium granulate [32], and MgAl–CO_3–LDH [67], were clearly lower than those of As(V) at all pH levels. The discrepancy between As(V) and As(III) removal by aluminium-based absorbents could be attributed to a weaker affinity between As(III) and Al-based hydroxyl groups on the surface of the solids [31,32]. In the pH range of the experiments, the uptake of arsenic increased with increasing pH until reaching the maximum adsorption and then decreased with further increases in pH in our experiments, as shown in Fig. 6. For the As(V) adsorption, there is a sharp maximum adsorption at the pH value of approximately 5.0, which is similar to the As(V) adsorption on cerium oxide modified activated carbon [13]. However, for the As(III) adsorption, the maximum adsorption is broad, occurring in the pH range of approximately 5.0–7.0. The Al-based hydroxyl groups on the adsorbent may play a key role in the arsenic removal via the ligand exchange mechanism.

Table 4
Langmuir isotherm parameters for arsenate and arsenite adsorption on Fe-modified molecular sieves

Parameters	q_m (mg/kg)	b (L/mg)	R^2
As(V)	666.67	1.071	0.9776
As(III)	232.56	0.768	0.9751

The pH-dependent behavior of arsenic adsorption by fly ash could be attributed to the synergistic effects of several competing factors that control the adsorption reaction between arsenic and the absorbents. Several mechanisms of arsenic removal by adsorbents from an aqueous medium have been proposed, including: (1) inner-sphere surface complexation, (2) outer-sphere surface complexation (i.e., electrostatic interaction), (3) surface precipitation, and (4) intercalation by reconstruction of the structure on the adsorbent surface [33,63,66,68]. During the formation of the surface complexes, electrostatic attraction or repulsion of the aqueous arsenate or arsenite species with the surface of the adsorbent largely control the migration of oxyanions to the surface of the adsorbent, which is the prerequisite of the adsorption reaction [69]. Herein, arsenic adsorption on the adsorbents was governed by the joint effects of pH of the point of zero charge (pHpzc) of the adsorbents and the speciation of aqueous As(V) and As(III).

The degree of protonation of As(V) and As(III) anions in an aqueous solution is influenced by the pH. At pH < 2, H_3AsO_4 is the main form of the As(V) species, whereas $H_2AsO_4^-$ becomes the dominant species in the pH range of 3–6. It is also well known that the adsorbent surface is protonated, and the surface change is positive at pH below pH_{PZC}. However, the adsorbent surface is deprotonated, and

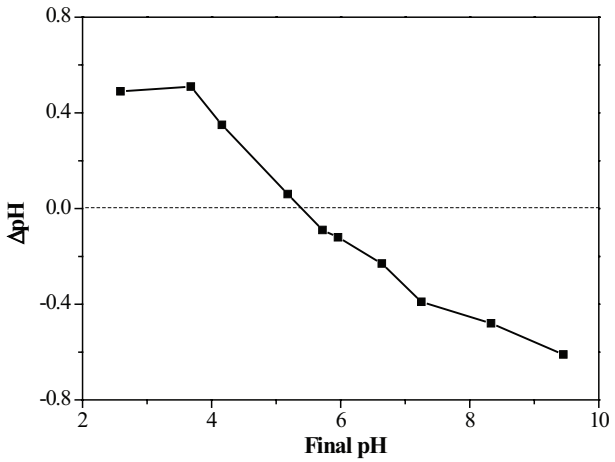

Fig. 7. Point of zero charge of the fly ash.

the surface change could be negative when the solution pH is above pH_{PZC}. With the increase of the pH, the change of the surface charge not only results in decreased electrostatic attraction or increased electrostatic repulsion between the adsorbents and anionic arsenic species but also leads to the decrease in the mass transfer of arsenic toward the adsorbent surface. As shown in Fig. 7, the pH_{PZC} value of fly ash is approximately 5.4. Therefore, below the pH_{PZC} of 5.4, the surface of the fly ash is positively charged, which is normally favorable for the adsorption of the negatively charged anionic species ($H_2AsO_4^-$ anions in this experiment). On the other hand, above the pH_{PZC} 5.4, the surface of the adsorbent becomes more negatively charged and the dominant As(V) species are $HAsO_4^{2-}$ in the pH range of 6–9. Herein, electrostatic repulsion between the adsorbents and anionic arsenic species becomes stronger and the rate of the arsenic species migration to the adsorbent surface is reduced. As a result of above reasons, the arsenate adsorption by fly ash increased with increasing pH and have a sharp maximum adsorption obtained at the pH of approximately 5.0, followed by the decrease in the adsorption upon further increases in pH.

Different from arsenate, the dominant aqueous arsenite species are H_3AsO_3 at pH < ~9 and $H_2AsO_3^-$ at pH 9–12 [1]. At pH < ~9, the neutral H_3AsO_3 molecule is the dominant arsenite species. This may be the cause of the difference between As(V) and As(III) adsorption on fly ash. Arsenite adsorption onto the aluminium hydroxyl surface of fly ash through ligand exchange reactions at pH < ~9 is depicted schematically below (≡[Al] represents the adsorption sites on the surface of fly ash):

$$\equiv[\mathrm{Al-OH}](s) + H_3AsO_3 \rightarrow \equiv \mathrm{Al-O_2As(OH)^-} + 2H^+ \quad (3)$$

$$\equiv[\mathrm{Al-OH}](s) + H_3AsO_3 \rightarrow \equiv \mathrm{Al-O_2AsO^{2-}} + 3H^+ \quad (4)$$

Since arsenite is present predominantly as a neutral molecule at pH < ~9, the electrostatic attraction or repulsion does not play an important role, and the deprotonation of H_3AsO_3 is the rate-limiting step of the reaction. When pH increases from 3 to 7, the deprotonation process of the neutral arsenite molecules is promoted and plays a major role in the adsorption process of arsenite. As a result of the change of adsorbent surface charge and improvement of arsenite deprotonation, the arsenite adsorption is enhanced and a broad adsorption maximum emerges in the pH range of approximately 5.0–7.0. At pH > ~7, and the electrostatic repulsion between the negatively charged surface and anionic arsenite species leads to decreased adsorption with further increases in the pH.

4. Conclusion

In summary, the performance of coal fly ash for arsenate and arsenite removal was investigated by batch experiments to reduce environmental hazards and realize high-value utilization of coal fly ash. Langmuir adsorption isotherms indicated that the maximum adsorption capacities of As(V) and As(III) at pH 5.0 were 666.67 and 232.56 mg/kg, respectively. The uptake of arsenic species was highly affected by solution pH, and the uptake of As(V) by fly ash was remarkably higher than that of As(III) under the same conditions, with respect to the same pH. Thus, the use of coal fly ash to treat arsenic pollution may be an effective method for industrial waste reuse. However, the relatively lower specific surface areas and arsenic adsorption capacities likely restrict the utilization of coal fly ash on arsenic wastewater treatments. Further studies are needed to enhance the adsorption capability of fly ash by methods such as modification, heat and/or acid treatment, and zeolitization.

Acknowledgement

This work was financially supported by the National Natural Science Foundation of China (Nos. 41530643 and 41807358) and the Strategic Priority Research Program of the Chinese Academy of Sciences (No. XDB14020203).

References

[1] P.L. Smedley, D.G. Kinniburgh, A review of the source, behaviour and distribution of arsenic in natural waters, Appl. Geochem., 17 (2002) 517–568.
[2] D. Mohan, C.U. Pittman, Jr., Arsenic removal from water/wastewater using adsorbents–A critical review, J. Hazard. Mater., 142 (2007) 1–53.
[3] V.K. Gupta, I. Ali, Environmental Water: Advances in Treatment, Remediation and Recycling, 2012.
[4] A.T. Hubbard, Encyclopedia of Surface and Colloid Science, Marcel Dekker, New York, 2004.
[5] A.A. Basheer, Chemical chiral pollution: impact on the society and science and need of the regulations in the 21st century, Chirality, 30 (2017) 402–406.
[6] I. Ali, H.Y. Aboulenein, V.K. Gupta, Nano Chromatography and Capillary Electrophoresis: Pharmaceutical and Environmental Analyses, 2009.
[7] I. Ali, H.Y. Aboulenein, Instrumental methods in metal ion speciation, Chromatogr. Sci. Ser., 388 (2006) 869–870.
[8] V.K. Sharma, M. Sohn, Aquatic arsenic: toxicity, speciation, transformations, and remediation, Environ. int., 35 (2009) 743–759.
[9] L. Rodriguez-Lado, G. Sun, M. Berg, Q. Zhang, H. Xue, Q. Zheng, C.A. Johnson, Groundwater arsenic contamination throughout China, Science, 341 (2013) 866–868.
[10] S. Dixit, J.G. Hering, Comparison of arsenic(V) and arsenic(III) sorption onto iron oxide minerals: implications for arsenic mobility, Environ. Sci. Technol., 37 (2003) 4182–4189.

[11] G. Zhang, J. Qu, H. Liu, R. Liu, R. Wu, Preparation and evaluation of a novel Fe-Mn binary oxide adsorbent for effective arsenite removal, Water. Res., 41 (2007) 1921–1928.
[12] H. Zhu, Y. Jia, X. Wu, H. Wang, Removal of arsenic from water by supported nano zero-valent iron on activated carbon, J. Hazard. Mater., 172 (2009) 1591–1596.
[13] Y. Yu, C. Zhang, L. Yang, J. Paul Chen, Cerium oxide modified activated carbon as an efficient and effective adsorbent for rapid uptake of arsenate and arsenite: material development and study of performance and mechanisms, Chem. Eng. J., 315 (2017) 630–638.
[14] D. Lakshmanan, D.A. Clifford, G. Samanta, Comparative study of arsenic removal by iron using electrocoagulation and chemical coagulation, Water. Res., 44 (2010) 5641–5652.
[15] L.C. Roberts, S.J. Hug, T. Ruettimann, M. Billah, A.W. Khan, M.T. Rahman, Arsenic removal with iron(II) and iron(III) waters with high silicate and phosphate concentrations, Environ. Sci. Technol., 38 (2004) 307–315.
[16] I. Ali, V.K. Gupta, Advances in water treatment by adsorption technology, Nat. Protoc., 1 (2006) 2661–2667.
[17] I. Ali, H.Y. Aboulenein, Speciation of arsenic and chromium metal ions by reversed phase high performance liquid chromatography, Chemosphere, 48 (2002) 275–278.
[18] I. Ali, Z.A. Al-Othman, A. Alwarthan, M. Asim, T.A. Khan, Removal of arsenic species from water by batch and column operations on bagasse fly ash, Environ. Sci. Pollut. Res., 21 (2014) 3218–3229.
[19] I. Ali, T.A. Khan, M. Asim, Removal of arsenate from groundwater by electrocoagulation method, Environ. Sci. Pollut. Res., 19 (2012) 1668–1676.
[20] I. Ali, Z.A. Al-Othman, A. Alwarthan, Molecular uptake of congo red dye from water on iron composite nano particles, J. Mol. Liq., 224 (2016) 171–176.
[21] E.A. Burakova, I. Ali, T.P. Dyachkova, A.V. Rukhov, E.N. Tugolukov, E.V. Galunin, A.G. Tkachev, A.A. Basheer, Novel and economic method of carbon nanotubes synthesis on a nickel magnesium oxide catalyst using microwave radiation, J. Mol. Liq., 253 (2018) 340–346.
[22] I. Ali, O.M.L. Alharbi, Z.A. Alothman, A.Y. Badjah, A. Alwarthan, A.A. Basheer, Artificial neural network modelling of amido black dye sorption on iron composite nano material: kinetics and thermodynamics studies, J. Mol. Liq., 250 (2018) 1–8.
[23] I. Ali, Z.A. Alothman, M.M. Sanagi, Green synthesis of iron nano-impregnated adsorbent for fast removal of fluoride from water, J. Mol. Liq., 211 (2015) 457–465.
[24] O.M.L. Alharbi, A.A. Basheer, R.A. Khattab, I. Ali, Health and environmental effects of persistent organic pollutants, J. Mol. Liq., 263 (2018) 442–453.
[25] I. Ali, New generation adsorbents for water treatment, Chem. Rev., 112 (2012) 5073–5091.
[26] I. Ali, Z.A. Alothman, A. Alwarthan, Supra molecular mechanism of the removal of 17-β-estradiol endocrine disturbing pollutant from water on functionalized iron nano particles, J. Mol. Liq., 241 (2017) 123–129.
[27] I. Ali, Z.A. Alothman, A. Alwarthan, Uptake of propranolol on ionic liquid iron nanocomposite adsorbent: kinetic, thermodynamics and mechanism of adsorption, J. Mol. Liq., 236 (2017) 205–213.
[28] M.H. Dehghani, D. Sanaei, I. Ali, A. Bhatnagar, Removal of chromium(VI) from aqueous solution using treated waste newspaper as a low-cost adsorbent: kinetic modeling and isotherm studies, J. Mol. Liq., 215 (2016) 671–679.
[29] Y.F. Jia, G.P. Demopoulos, Adsorption of arsenate onto ferrihydrite from aqueous solution: influence of media (sulfate vs nitrate), added gypsum, and pH alteration, Environ. Sci. Technol., 39 (2005) 9523–9527.
[30] W. Li, C.Y. Cao, L.Y. Wu, M.F. Ge, W.G. Song, Superb fluoride and arsenic removal performance of highly ordered mesoporous aluminas, J. Hazard. Mater., 198 (2011) 143–150.
[31] J. Mertens, B. Casentini, A. Masion, R. Pothig, B. Wehrli, G. Furrer, Polyaluminum chloride with high Al30 content as removal agent for arsenic-contaminated well water, Water. Res., 46 (2012) 53–62.
[32] J. Mertens, J. Rose, R. Kagi, P. Chaurand, M. Plotze, B. Wehrli, G. Furrer, Adsorption of arsenic on polyaluminum granulate, Environ. Sci. Technol., 46 (2012) 7310–7317.
[33] X. Gao, R.A. Root, J. Farrell, W. Ela, J. Chorover, Effect of silicic acid on arsenate and arsenite retention mechanisms on 6-L ferrihydrite: a spectroscopic and batch adsorption approach, Appl. Geochem., 38 (2013) 110–120.
[34] G. Neupane, R.J. Donahoe, Y. Arai, Kinetics of competitive adsorption/desorption of arsenate and phosphate at the ferrihydrite–water interface, Chem. Geol., 368 (2014) 31–38.
[35] P.J. Swedlund, H. Holtkamp, Y. Song, C.J. Daughney, Arsenate-ferrihydrite systems from minutes to months: a macroscopic and ir spectroscopic study of an elusive equilibrium, Environ. Sci. Technol., 48 (2014) 2759–2765.
[36] I. Ali, Z.A. Alothman, A. Al-Warthan, Sorption, kinetics and thermodynamics studies of atrazine herbicide removal from water using iron nano-composite material, Int. J. Environ. Sci. Te., 13 (2016) 733–742.
[37] I. Ali, Z.A. Al-Othman, A. Alwarthan, Green synthesis of functionalized iron nano particles and molecular liquid phase adsorption of ametryn from water, J. Mol. Liq., 221 (2016) 1168–1174.
[38] I. Ali, Z.A. Alothman, A. Alwarthan, Removal of secbumeton herbicide from water on composite nanoadsorbent, Desal. Wat, Treat, 57 (2016) 1–13.
[39] I. Ali, Z.A. Al-Othman, A. Alwarthan, Synthesis of composite iron nano adsorbent and removal of ibuprofen drug residue from water, J. Mol. Liq., 219 (2016) 858–864.
[40] I. Ali, Z.A. Al-Othman, O.M.L. Alharbi, Uptake of pantoprazole drug residue from water using novel synthesized composite iron nano adsorbent, J. Mol. Liq., 218 (2016) 465–472.
[41] Ali, Asim, Mohd, Khan, A. T., Arsenite removal from water by electro-coagulation on zinc-zinc and;copper-copper electrodes, Int. J. Environ. Sci. Technol., 10 (2013) 377–384.
[42] S.E. O'Reilly, D.G. Strawn, D.L. Sparks, Residence time effects on arsenate adsorption/desorption mechanisms on goethite, Soil. Sci. Soc. Am. J., 65 (2001) 67–77.
[43] S. Kashiwakura, H. Ohno, K. Matsubae-Yokoyarna, Y. Kumagai, H. Kubo, T. Nagasaka, Removal of arsenic in coal fly ash by acid washing process using dilute H_2SO_4 solvent, J. Hazard. Mater., 181 (2010) 419–425.
[44] A. Deonarine, A. Kolker, A.L. Foster, M.W. Doughten, J.T. Holland, J.D. Bailoo, Arsenic speciation in Bituminous Coal Fly Ash and transformations in response to redox conditions, Environ. Sci. Technol., 50 (2016) 6099–6106.
[45] L. Ruhl, A. Vengosh, G.S. Dwyer, H. Hsu-Kim, A. Deonarine, M. Bergin, J. Kravchenko, Survey of the potential environmental and health impacts in the immediate aftermath of the coal ash spill in Kingston, Tennessee, Environ. Sci. Technol., 43 (2009) 6326–6333.
[46] L. Ruhl, A. Vengosh, G.S. Dwyer, H. Hsu-Kim, A. Deonarine, Environmental impacts of the coal ash spill in Kingston, Tennessee: an 18-month survey, Environ. Sci. Technol., 44 (2010) 9272–9278.
[47] A. Deonarine, G. Bartov, T.M. Johnson, L. Ruhl, A. Vengosh, H. Hsu-Kim, Environmental impacts of the Tennessee Valley Authority Kingston coal ash spill. 2. Effect of coal ash on methylmercury in historically contaminated river sediments, Environ. Sci. Technol., 47 (2013) 2100–2108.
[48] E. Soco, J. Kalembkiewicz, Removal of copper(II) and zinc(II) ions from aqueous solution by chemical treatment of coal fly ash, Croat. Chem. Acta, 88 (2015) 267–279.
[49] C. An, S. Yang, G. Huang, S. Zhao, P. Zhang, Y. Yao, Removal of sulfonated humic acid from aqueous phase by modified coal fly ash waste: equilibrium and kinetic adsorption studies, Fuel, 165 (2016) 264–271.
[50] X. Deng, L. Qi, Y. Zhang, Experimental study on adsorption of hexavalent chromium with microwave-assisted alkali modified fly ash, Water. Air. Soil. Pollut., 229 (2018) 18.
[51] B. Wang, Y. Zhou, L. Li, H. Xu, Y. Sun, Y. Wang, Novel synthesis of cyano-functionalized mesoporous silica nanospheres (MSN) from coal fly ash for removal of toxic metals from wastewater, J. Hazard. Mater., 345 (2018) 76–86.

[52] S.B. Wang, M. Soudi, L. Li, Z.H. Zhu, Coal ash conversion into effective adsorbents for removal of heavy metals and dyes from wastewater, J. Hazard. Mater., 133 (2006) 243–251.
[53] K. Styszko, J. Szczurowski, N. Czuma, D. Makowska, M. Kistler, Ł. Uruski, Adsorptive removal of pharmaceuticals and personal care products from aqueous solutions by chemically treated fly ash, Int. J. Environ. Sci. Technol., 15 (2018) 493–506.
[54] H. Jin, Y. Liu, C. Wang, X. Lei, M. Guo, F. Cheng, M. Zhang, Two-step modification towards enhancing the adsorption capacity of fly ash for both inorganic Cu(II) and organic methylene blue from aqueous solution, Environ. Sci. Pollut. Res., 25 (2018) 36449–35461.
[55] N. Wang, Q. Zhao, H. Xu, W. Niu, L. Ma, D. Lan, L. Hao, Adsorptive treatment of coking wastewater using raw coal fly ash: adsorption kinetic, thermodynamics and regeneration by Fenton process, Chemosphere, 210 (2018) 624–632.
[56] A.P. Khodadoust, T.L. Theis, I.P. Murarka, P. Naithani, K. Babaeivelni, Uptake of arsenic by alkaline soils near alkaline coal fly ash disposal facilities, Environ. Monit. Assess., 185 (2013) 10339–10349.
[57] A. Adamczuk, D. Kolodynska, Equilibrium, thermodynamic and kinetic studies on removal of chromium, copper, zinc and arsenic from aqueous solutions onto fly ash coated by chitosan, Chem. Eng. J., 274 (2015) 200–212.
[58] A.K. Meher, S. Das, S. Rayalu, A. Bansiwal, Enhanced arsenic removal from drinking water by iron-enriched aluminosilicate adsorbent prepared from fly ash, Desal. Wat. Treat, 57 (2016) 20944–20956.
[59] K. Zhang, D. Zhang, Arsenic removal from water using a novel amorphous adsorbent developed from coal fly ash, Water. Sci. Technol., 73 (2016) 1954–1962.
[60] H. Sri, F.F. Hanum, A. Takeyama, S. Kambara, Effect of additives on arsenic, boron and selenium leaching from coal fly ash, Minerals, 7 (2017) 99.
[61] L. Xu, Z. Zhao, S. Wang, R. Pan, Y. Jia, Transformation of arsenic in offshore sediment under the impact of anaerobic microbial activities, Water. Res., 45 (2011) 6781–6788.
[62] Z. Yuan, S. Wang, X. Ma, X. Wang, G. Zhang, Y. Jia, W. Zheng, Effect of iron reduction by enolic hydroxyl groups on the stability of scorodite in hydrometallurgical industries and arsenic mobilization, Environ. Sci. Pollut. Res., 24 (2017) 26534–26544.
[63] Y. Jia, L. Xu, X. Wang, G.P. Demopoulos, Infrared spectroscopic and X-ray diffraction characterization of the nature of adsorbed arsenate on ferrihydrite, Geochim. Cosmochim. Acta, 71 (2007) 1643–1654.
[64] J. Zhu, Z. Lou, Y. Liu, R. Fu, S.A. Baig, X. Xu, Adsorption behavior and removal mechanism of arsenic on graphene modified by iron–manganese binary oxide ($FeMnO_x$/RGO) from aqueous solutions, RSC. Adv., 5 (2015) 67951–67961.
[65] Y. Li, F.S. Zhang, F.R. Xiu, Arsenic (V) removal from aqueous system using adsorbent developed from a high iron-containing fly ash, Sci. Total. Environ., 407 (2009) 5780–5786.
[66] D. Zhang, Y. Jia, J. Ma, Z. Li, Removal of arsenic from water by Friedel's salt (FS: $3CaO{\cdot}Al_2O_3{\cdot}CaCl_2{\cdot}10H_2O$), J. Hazard. Mater., 195 (2011) 398–404.
[67] L. Yang, Z. Shahrivari, P.K.T. Liu, M. Sahimi, T.T. Tsotsis, Removal of trace levels of arsenic and selenium from aqueous solutions by calcined and uncalcined layered double hydroxides (LDH), Ind. Eng. Chem. Res., 44 (2005) 6804–6815.
[68] K.H. Goh, T.T. Lim, Z. Dong, Application of layered double hydroxides for removal of oxyanions: a review, Water. Res., 42 (2008) 1343–1368.
[69] A. Jain, K.P. Raven, R.H. Loeppert, Arsenite and arsenate adsorption on ferrihydrite: surface charge reduction and net OH^- release stoichiometry, Environ. Sci. Technol., 33 (1999) 1179–1184.